Bull. Disas. Prev. Res. Inst., Kyoto Univ., Vol. 20, Part 3, No. 176, March, 1971 127

On the Oscillatory Flow in Turbulent Boundary Layers Induced by Water Waves

By Hideaki NODA

(Manuscript received December 19, 1970)

Abstract

A method is presented for calculating various characteristics of the turbulent boundary layers developed on both smooth and rough bottoms by waves. The profiles of velocities and the mass transport velocities in the oscillating turbulent boundary layer are derived theoretically on the basis of a physically meaningful assumption of an eddy viscosity, and the numerical results are compared with existing experimental data which have been done by others.

In addition, the analytical data on the oscillatory flow near the bottom are applied to a theoretical description of some of the problems of sediment movement such as determination of the predominant direction of sediment transport due to waves.

1. Introduction

In order to estimate accurately the magnitude and the predominant direction of sediment transport, it is important to find a law which describes the oscillatory flow near the bottom due to surface waves and from which the hydrodynamic forces acting on the sand grains can be derived, and to reveal a relationship between the flow near the bottom and the movement of sediment. Much theoretical and experimental studyhas been done by others on the action of laminar boundary layers under the surface waves. Longuet-Higgins[1] have deseribed the mechanics of the boundary layers which are developed on bottoms by a progressive wave in shallow water. Iwagaki and Tsuchiya[2] have studied theoretically and experimentally the problem of wave decay in shallow water due to bottom friction under the surface waves. However, the mechanics of the turbulent boundary layers under the waves are not well understood because of the complexity of the phenomena and because of the difficulty of developing turbulent boundary layers due to waves in small-scale laboratory flumes.

To observe the characteristics of turbulent boundary layers due to oscillatory flow, Kalkanis[3] experimented using an apparatus with an oscillating solid boundary. Jonsson[4] conducted experiments using a U-type wave tunnel in order to measure the velocity in the turbulent oscillatory flow. Recently, Horikawa and Watanabe[5] have shown that the velocities in the turbulent boundary layer under waves developed on bottoms can be measured by the flow visualization method.

On the other hand, Kajiura[6] has presented a theoretical model of the structure of the turbulent oscillatory flow in which the basic idea was to consider the average state of turbulence over one wave period and then to assume an eddy viscosity analogous to that for steady turbulent flow. And Johns[7] has shown a boundary layer method for the determination of viscous wave damping in turbulent conditions by assuming an eddy viscosity different from that of Kajiura.

In the present paper, the velocity distribution and the bottom shear stress in the turbulent boundary layers developed on both smooth and rough bottoms are estimated by using an assumption of eddy viscosity similar to that of Johns. In addition the mass transport velocity in the oscillating turbulent boundary layers under partial reflected waves is also derived on the basis of this theory.

This theory suggests that the direction of the net sediment transport is affected by the mass transport.

2. Analytical Considerations of Velocity Profiles in Turbulent Boundary Layers

The objective of the present study is to derive an adequate description of the turbulent flow of a realfluid near smooth and rough bottoms under wave action.

(1) Formulation

For a two-dimensional case, taking the coordinate axes (x, z) fixed in the horizontal bottom with the x-axis directed horizontally and the z-axis vertically, and assuming an incompressible homogeneous fluid of constant depth, the boundary layer equation for the averaged motion is:

$$\frac{\partial u}{\partial t}+u\frac{\partial u}{\partial x}+w\frac{\partial u}{\partial z}=-\frac{1}{\rho}\frac{\partial p}{\partial x}+\frac{1}{\rho}\frac{\partial \tau}{\partial x} \tag{1}$$

and the equation of continuity for the incompressible fluid is given by the expression:

$$\frac{\partial u}{\partial x}+\frac{\partial w}{\partial z}=0 \tag{2}$$

in which p is the pressure, ρ the density, τ the shear stress, u and w the averaged velocity components in the boundary layer in the direction of x and z, respectively. Additionally, u_∞ denotes the velocity just outside the boundary layer, and it is related to the pressure in Eq. (1) by the form

$$-\frac{1}{\rho}\frac{\partial p}{\partial x}=\frac{\partial u_\infty}{\partial t}+u_\infty\frac{\partial u_\infty}{\partial x} \tag{3}$$

In dealing with the turbulent case, an appropriate expression must be proposed for the shear stress of turbulent flow. The shear stress is given by the expression

$$\frac{\tau}{\rho}=N_z\frac{\partial u}{\partial z} \tag{4}$$

where N_z is usually referred to in the literature as the coefficient of the eddy viscosity. In addition, it is assumed that the coefficient of the eddy viscosity N_z is a function of z only and is given by the form

$$N_z=\nu N(z) \tag{5}$$

where ν is the kinematic viscosity and $N(z)$, which is a non-dimensional form, describes the effect of turbulence.

The boundary conditions are that

$$u=w=0 \quad \text{at} \quad z=0 \tag{6}$$

$$u=u_\infty \quad \text{as} \quad z\to\infty \tag{7}$$

The velocity u is taken to be equivalent to that of the bottom in the irrotational theory, that is,

$$u_\infty=\varepsilon u_{\infty 1}+\varepsilon^2 u_{\infty 1}+\cdots\cdots \tag{8}$$

where ε is a small ordering parameter, $\omega=2\pi/T$ (T: the wave period), $u_{\infty 1}$ and $u_{\infty 2}$

are expressed by the real part of

$$\left.\begin{array}{ll} u_{b1}(x)\, e^{i\omega t} & \\ \text{and} \quad u_{b2}(x)\, e^{i\omega t} & \end{array}\right\} \tag{9}$$

respectively.

The vertical velocity in the boundary layer is derived from Eqs. (2) and (6) in the form

$$w = -\frac{\delta}{\alpha}\int_{\xi_0}^{\xi} \frac{\partial u}{\partial x}\, d\xi \tag{10}$$

by introducing a non-dimensional quantity ξ defined as follows:

$$\xi = \xi_0 + \alpha\left(\frac{z}{\delta}\right) \tag{11}$$

where

$$\delta = (\nu T/2\pi)^{1/2}$$
$$\xi_0 = 1+\alpha\ (z_0/\delta) \tag{12}$$

α is a constant and z_0 the roughness length.

Substituting Eqs. (3), (4), (5) and (10) into Eq. (1) yields

$$\frac{\partial u}{\partial t} + u\frac{\partial u}{\partial x} - \frac{\partial u}{\partial \xi}\int_{\xi_0}^{\xi}\frac{\partial u}{\partial x}\, d\xi = \frac{\partial u_\infty}{\partial t} + u_\infty\frac{\partial u_\infty}{\partial x} + \alpha^2\omega\frac{\partial}{\partial \xi}\left(N\frac{\partial u}{\partial \xi}\right) \tag{13}$$

If the horizontal velocity in the boundary layer is expanded as a power series in ε in the form

$$u = \varepsilon u_1 + \varepsilon^2 u_2 + \cdots\cdots\cdots \tag{14}$$

the differential equation of the first approximation for u is given by the expression

$$\frac{\partial u_1}{\partial t} = \frac{\partial u_{\infty 1}}{\partial t} + \alpha^2\omega\frac{\partial}{\partial \xi}\left(N\frac{\partial u_1}{\partial \xi}\right) \tag{15}$$

with the boundary conditions

$$\left.\begin{array}{ll} u_1 = 0 & \text{at} \quad \xi = \xi_0 \\ u_1 = u_{\infty 1} & \text{as} \quad \xi \to \infty \end{array}\right\} \tag{16}$$

By putting a solution for u_1

$$u_1 = u_{b1}(x)\,[1 - F(\xi)]e^{i\omega t} \tag{17}$$

and by substituting Eqs. (9) and (17) into Eq. (15), the differential equation for the function F is obtained as follows:

$$\frac{d}{d\xi}\left(N\frac{dF}{d\xi}\right) - \frac{i}{\alpha^2}F = 0 \tag{18}$$

with the boundary conditions

$$\left.\begin{array}{l} F(\xi_0) = 1 \\ F(\infty) = 0 \end{array}\right\} \tag{19}$$

The velocity u_1 in the boundary layer is expressed by the real part of Eq. (17).

The foregoing formulation is quite general, but the boundary layer equation for Kalkanis's experiment which was done by using an oscillating bed takes the form

$$\frac{\partial u}{\partial t} = \frac{1}{\rho}\frac{\partial \tau}{\partial z} \tag{20}$$

with the boundary conditions

$$\left.\begin{array}{ll} u = u_\infty & \text{at} \quad z = 0 \\ \text{and} \quad u = 0 & \text{as} \quad z \to \infty \end{array}\right\} \tag{21}$$

where u_∞ is a periodic function of t only. Therefore, a solution for u is obtained in the form

$$u=u_\infty F\ (\xi) \tag{22}$$

by substituting Eqs. (4) and (5) into Eq. (20). Additionally, that of Jonsson's experiment which was done by using a water tunnel is given by Eq. (15), but the term $(\partial u_{\infty 1}/\partial t)$ is independent of any spatial coordinate. Therefore, its solution is expressed by Eq. (17) with u_{b1} = constant.

(2) Analytical solution of equations

Non-dimensional form of the eddy viscosity N: The functional form of N must be determined in order to derive the velocity profile of the oscillatory flow in the turbulent boundary layers.

Kajiura[6] assumed the turbulent boundary layer of the oscillatory flow to consist of three parts: the inner layer, the overlap layer, and the outer layer, by following the concept of the wall and the defect layers established for the case of an unidirectional turbulent boundary layer. Consequently, eddy viscosity was assumed to be constant in the inner and outer layers, and to increase in proportion to the height z above the bottom in the overlap layer. Such an assumption was employed by Johns[7] in problems of damping of gravity waves and tides. However, the eddy viscosity which was assumed by Johns increases and decreases with z^2 in the inner and the overlap layer, respectively, and is constant in the outer layer. Kalkanis also showed that the eddy viscosity for the case of the turbulent boundary layer of oscillating beds was assumed to be proportional to z^2.

In this paper, by following a concept similar to that of Johns (1968), and by taking account of the bottom roughness, the non-dimensional form of the eddy viscosity N is assumed in the form:

$$N=\begin{cases}\xi^2 & \text{for} \quad \xi_0\leq\xi\leq\xi_1 & (23)\\ \zeta^2 & \text{for} \quad \xi_1\leq\xi\leq\xi_2 & (24)\\ 1 & \text{for} \quad \xi_2\leq\xi & (25)\end{cases}$$

where

$$\zeta=1+\{(\xi_1-1)(\xi_2-\xi)/(\xi_2-\xi_1)\} \tag{26}$$

and

$$\left.\begin{aligned}\xi_1&=\xi_0+\alpha\ (z_1/\delta)\\ \xi_2&=\xi_0+\alpha\ (z_2/\delta)\end{aligned}\right\} \tag{27}$$

and z_0 is the roughness length, but is not well defined physically. The quantities α, z_1 and z_2 are disposable parameters which should be determined by the turbulent structure and the scale length of the boundary layer.

For the case of a smooth bottom, the eddy viscosity is given by putting $z_0=0$ in Eqs. (23)$\sim$(25).

Finally, because of dividing the oscillating turbulent boundary layer into three parts, the boundary conditions which must be added in Eq. (19) are that F and $dF/d\xi$ are individually continuous at $\xi=\xi_1$ and $\xi=\xi_2$.

Solution for $\xi_0\leq\xi\leq\xi_1$:

Substituting Eq. (23) into Eq. (18) gives the differential equation for F:

$$\left.\begin{aligned} &\frac{d}{d\xi}\left(\xi^2\frac{dF}{d\xi}\right)-\frac{i}{\alpha^2}F=0 \\ \text{or}\quad &\xi^2\frac{d^2F}{d\xi^2}+2\xi\frac{dF}{d\xi}-\frac{i}{\alpha^2}F=0 \end{aligned}\right\} \tag{28}$$

and hence its solution is given by :

$$F=\xi^{-1/2}(A_1\xi^{-n}+A_2\xi^n) \tag{29}$$

in which A_1 and A_2 are constants determined by the boundary conditions and n $(=n_R+in_I)$ is a complex constant in the form

$$n=\left(\frac{1}{4}+\frac{i}{\alpha^2}\right)^{1/2} \tag{30}$$

as a function of α.

Thus, n_R and n_I which are the real and the imaginary parts of n, respectively, can be expressed as follows :

$$n_R=\left(\frac{\sqrt{1+(2/\alpha)^4}+1}{8}\right)^{1/2} \tag{31}$$

$$n_I=\left(\frac{\sqrt{1+(2/\alpha)^4}-1}{8}\right)^{1/2} \tag{32}$$

Solution for $\xi_1\leq\xi\leq\xi_2$:

For Eq. (26), it is readily seen that

$$\frac{d\zeta}{d\xi}=-\beta \tag{33}$$

by putting

$$\beta=-\frac{\xi_1-1}{\xi_2-\xi_1} \tag{34}$$

Substituting Eqs. (24) and (33) into Eq. (18) gives the differential equation for F :

$$\frac{d}{d\zeta}\left(\zeta^2\frac{dF}{d\zeta}\right)-\frac{i}{\alpha_e{}^2}F=0 \tag{35}$$

with $\alpha_e=\alpha\beta$. Since Eq. (35) is the same form as Fq. (28), its solution is given by :

$$F=\xi^{-1/2}\,(B_1\,\zeta^{-m}+B_2\,\zeta^m) \tag{36}$$

in which B_1, B_2 and m $(=m_R+im_I)$ are complex contants, and then m is a function of α_e only ;

$$m=\left(\frac{1}{4}+\frac{i}{\alpha_e{}^2}\right)^{1/2} \tag{37}$$

Additionally,

$$m_R=\left(\frac{\sqrt{1+(2/\alpha_e)^2}+1}{8}\right)^{1/2} \tag{38}$$

$$m_I=\left(\frac{\sqrt{1+(2/\alpha_e)^2}-1}{8}\right)^{1/2} \tag{39}$$

Solution for $\xi_2\leq\xi$:

Since $N=1$ for $\xi\geq\xi_2$, then Eq. (18) is simplified in the form :

$$\frac{d^2F}{d\xi^2}-\frac{i}{\alpha^2}F=0 \tag{40}$$

and its solution is given by :

$$F=C\,\exp\left(-\frac{1+i}{2\sqrt{\alpha}}\,\xi\right) \tag{41}$$

where C is a constant.

Determination of the constants of intergration A_1, A_2, B_1, B_2 and C:

By applying the boundary conditions (19) and the continuous conditions of F and $dF/d\xi$ at $\xi=\xi_1$ and $\xi=\xi_2$, the constants of integration A_1, A_2, B_1, B_2 and C can be determined from the following equations:

$$(A_1\xi_0^{-n}+A_2\xi_0^{n})\ \xi_0^{-1/2}=1 \tag{42}$$

$$A_1\xi_1^{-n}+A_2\xi_1^{n}=B_1\xi_1^{-m}+B_2\xi_1^{m} \tag{43}$$

$$\beta\left\{\left(\frac{1}{2}+m\right)B_1\xi_1^{-m}+\left(\frac{1}{2}-m\right)B_2\,\xi_1^{m}\right\}$$
$$=-\left\{\left(\frac{1}{2}+n\right)A_1\xi_1^{-n}+\left(\frac{1}{2}-n\right)A_2\xi_1^{n}\right\} \tag{44}$$

$$\beta\left\{\left(\frac{1}{2}+m\right)B_1+\left(\frac{1}{2}-m\right)B_2\right\}=-\lambda Ce^{-\lambda\xi_2} \tag{45}$$

$$B_1+B_2=-\lambda Ce^{-\lambda\xi_2} \tag{46}$$

where

$$\lambda=\sqrt{i/\alpha^2}=(1+i)/\sqrt{2}\,\alpha \tag{47}$$

Hence, by using of Eqs. (45) and (46), it follows that

$$B_1=-D_1B_2 \tag{48}$$

where

$$D_1=\frac{(1+i)+\sqrt{2}\,\alpha_e\left(\frac{1}{2}-m\right)}{(1+i)+\sqrt{2}\,\alpha_e\left(\frac{1}{2}+m\right)} \tag{49}$$

Taking Eqs. (42) and (48) into account, Eqs. (43) and (44) may be written respectively:

$$A_2=\{(1-D_1\xi_1^{-2m})\,\xi_1^{m}B_2-\xi_1^{1/2}D_2^{-n}\}/2\xi_0^{n}\sinh(n\theta_2) \tag{50}$$

$$2n\xi_1^{n}A_2=\left[\left\{\left(\frac{1}{2}+m\right)\beta+\left(\frac{1}{2}+n\right)\right\}\left(1-D_1\xi_1^{-2m}\right)-2m\beta\right]\xi_1^{m}B_2, \tag{51}$$

in which

$$D_2=\xi_1/\xi_0 \qquad \text{and} \qquad \theta_2=\ln D_2 \tag{52}$$

Furthermore, by the combination of the above equations,

$$B_2=-B\xi_0^{1/2} \tag{53}$$

$$A_2=-A\xi_0^{1/2-n} \tag{54}$$

where the constants A and B are given by the following equations:

$$B=n/D_3\xi_1^{m} \tag{55}$$

$$A=\left[\left\{\left(\frac{1}{2}+m\right)\beta+\left(\frac{1}{2}+n\right)\right\}\left(1-D_1\xi_1^{-2m}\right)-2m\beta\right]/2D_2^{n}D_3 \tag{56}$$

by putting

$$D_3=\left[\left\{\left(\frac{1}{2}+m\right)\beta+\left(\frac{1}{2}+n\right)\right\}\left(1-D_1\xi_1^{-2m}\right)-2m\beta\right]\times$$
$$\sinh(n\theta_2)-nD_2^{n}\left(1-D_1\xi_1^{-2m}\right) \tag{57}$$

Hence, the insertion of these expressions in Eqs. (42), (48) and (46) yields

$$A_1=(1+A)\,\xi_0^{1/2}\xi_0^{n} \tag{58}$$

$$B_1=D_1B\xi_0^{1/2} \tag{59}$$

$$C=-(1-D_1)\,B\xi_0^{1/2} \tag{60}$$

Bottom shear stress

To clarify the relationship between bottom shear stress and wave characteristics such as the water particle velocity at bottoms u_∞, it is convenient to define

the following quantities :
the bottom friction velocity u_B*

$$\tau_B/\rho = u_0{}^* u_B{}^* \tag{61}$$

where u_0* is the amplitude of it. The velocity just outside the boundary layer $\varepsilon u_{\infty 1}$ is represented by the real part of

$$\varepsilon u_{b1}\ (x)\ e^{i\omega t}$$

If ϕ is the phase of u_B* relative to $\varepsilon u_{\infty 1}$, the bottom friction velocity u_B* is defined by

$$u_B{}^* = u_0{}^* e^{i(\omega t-\phi)} \tag{62}$$

Furthermore, the wave friction coefficient C_f is generally defined by

$$\tau_B/\rho = C_f\ (\varepsilon u_{b1})\ \varepsilon u_{\infty 1} \tag{63}$$

In general, by using Eq. (4), the bottom shear stress is given by

$$\tau_B/\rho = \left[N_z \frac{\partial u}{\partial z}\right] z=0 \tag{64}$$

The insertion of Eqs. (17) and (23) in Eq. (64) yields

$$\tau_B/\rho = (\nu/\delta)\ \varepsilon u_{b1}\ M\ (\xi_0)\ e^{i\omega t} \tag{65}$$

where

$$M(\xi_0) = -\alpha \xi_0 F'(\xi_0) \tag{66}$$

(3) Numerical Results and Comparison with Previous Experimental Data.

a) Comparison with experimental data obtained by Jonsson et al.

Jonsson measured the velocity distribution in an oscillating turbulent flow over an artificially roughened surface, by using a U-type water tunnel. The roughened surface used in his experiment was a triangular shape with the dimensions 0.6 cm high and 1.7cm apart, as shown in Figure 1. The velocity was measured by a small propeller (0.5cm diameter) and a photo-cell type current meter, and the bottom shear stress was calculated by the integration of the velocity distribution. In addition, Carlsen[8], later, experimenting on the same tunnel, added new data.

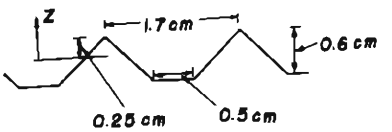

Fig. 1. Roughened surface used by Jonsson.

Their exprimental conditions are presented in Table 1.

Table 1. Experimental conditions used by Jonsson and Carlsen.

	Jonsson	Carlsen
wave height H (cm)	540	430
wave period T (sec)	8.39	7.20
water depth h (cm)	1000	1000
u_δ (cm/s)	213	153
δ (cm)	0.116	0.107
$u_\delta\delta/\nu$	2460	1640

Since εu_{b1} is constant in the case of the water tunnel, by putting $\varepsilon u_{b1} = u_0 \equiv \pi H/T \sinh kh$, Eq. (65) may be written in the form

$$\left.\begin{aligned} &\tau_B/\rho = u_0{}^2\ (u_0\delta/\nu)^{-1} M\ (\xi_0)\ e^{i\omega t} \\ \text{or}\quad &(\tau_B/\rho u_0{}^2)\ (u_0\delta/\nu) = M(\xi_0)\ e^{i\omega t} \end{aligned}\right\} \tag{67}$$

Hence, the relationship analogous to that of Eq. (62) becomes

$$(u_0^*/u_0)^2 e^{i(\omega t-\psi)} = (u_0\delta/\nu)^{-1} M e^{i\omega t} \tag{68}$$

By differentiating the above equation with respect to ωt, retaining the real part of it and putting $\omega t=\psi$, the phase difference ψ of τ_B relative to u_∞ is given in the form

$$\psi = \tan^{-1}(M_R/M_I) \tag{69}$$

where M_R and M_I are the real and imaginary parts of M, respectively.

To compare the experimental values with the theoretical prediction, the following method is adopted : firstly, $(\tau_B/\rho u_0^2)(u_0\delta/\nu)$ defined by Eq. (67) is com-

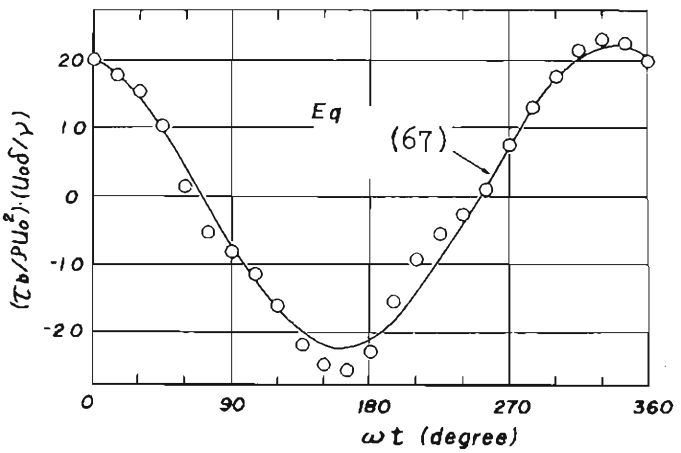

Fig. 2. Variation of bottom shear stress with time based on Jonsson's data.

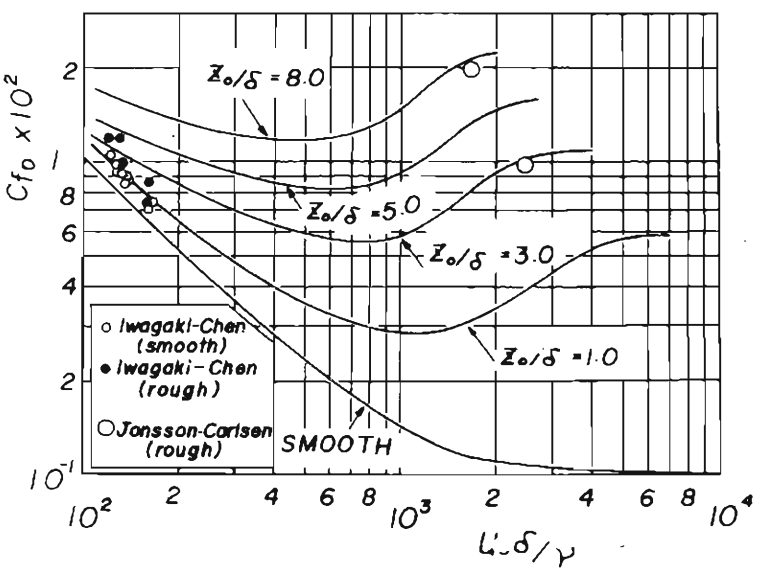

Fig. 3. Relationship between C_{f0} and R_e.

puted for the various values of α, z_0/δ, z_1/δ and z_2/δ ; secondly, the computed value is chosen so as to be in satisfactory agreement with the experimental data ; and finally, the numerical values of α, z_t/δ, z_1/δ are determined.

Figure 2 shows the variation of $(\tau_B/\rho u_0^2)$ $(u_0\delta/\nu)$ with time based on Jonsson's data. In this figure, the full line indicates the theoretical curve computed from Eq. (67) for a case of $\alpha=2.4$, $z_t/\delta=3.0$, $z_1/\delta=50$ and $z_t/\delta=100$. The agreement between the theory and the experiment is fairly good. In the comparison of the experimental data with the theoretical results, the Reynolds number, $u_0\delta/\nu=2460$, in this experiment seems to be roughly related to the parameter α with the values of 2.4.

From Eqs. (63) and (68), the maximum value C_{f0} of the friction coefficient C_f is given by

$$C_{f0}= (u_0\delta/\nu)^{-1}\mathrm{R}\,[Me^{i\phi}] \tag{70}$$

where the symbol R denotes the real part of $Me^{i\phi}$. Figure 3 shows the relationship between the maximum friction coefficient C_{f0} and the Reynolds number $u_0\delta/\nu$. In this figure, the full line denotes the theoretical curves computed from Eq. (70) as $\alpha=(u_0\delta/\nu)\times 10^{-3}$, and the experimental data of Jonsson, Carlsen and Iwagaki and Chen[9] are also plotted.

It is found from this figure that the value of α may be roughly equivalent to that of $(u_0\delta/\nu)\times 10^{-3}$, Furthermore, Nikuradse's roughness parameters used by Jonsson and Carlsen are 2.3 and 6.3cm, respectively, so that the roughness parameter of Carlsen is about 2.7 times that of Jonsson. As shown in Figure 3, in the present theory, Jonsson's and Carlsen's roughness parameters z_0/δ have the values of 3.0 and 8.0, respectively so that Carlsen's parameter is about 2.7 times that of Jonsson.

This shows that the theoretical predictions agree well with the experimental data. Figure 4 shows the variation with time of the velocity distribution in the turbulent boundary layer experimentally obtained by Jonsson. In this figure, the full lines denote the theoretical curves derived by Eqs. (29), (36) and (41), for

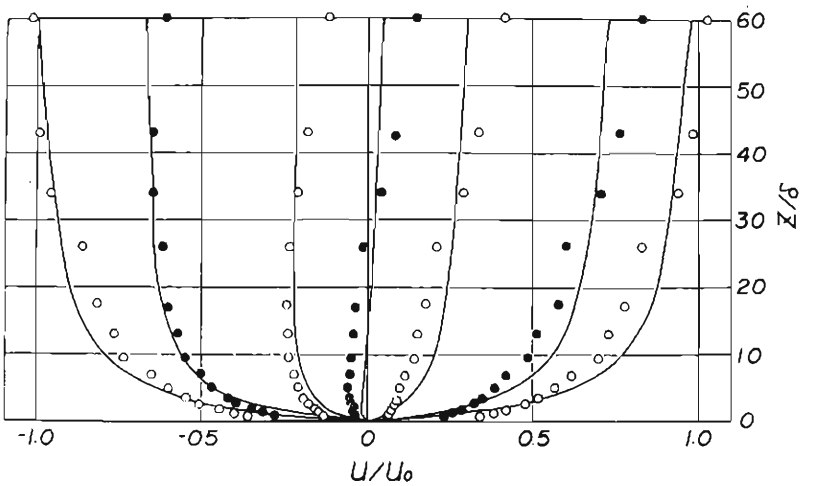

Fig. 4. Comparison on a velocity profile between experimental values and theoretical curves based on Jonsson's data.

the case of $\alpha=2.4$, $z_0/\delta=30$, $z_1/\delta=50$ and $z_2/\delta=100$. It is found that the observed values of u/u_0 almost agree with the theory except in the upper layer and furthermore, the thickness of the turbulent boundary layer is greater than that of the laminar case.

b) Comparison with experimental data obtained by Kalkanis

Table 2.

		Run 1	Run 2	Run 3
A_B	(ft)	1.0	1.5	1.5
T	(sec)	2.76	3.53	2.68
u_0	(ft/s)	2.275	2.67	3.52
ν	(ft^2/s)	1.06×10^{-5}	1.06×10^{-3}	1.06×10^{-5}
δ	(ft)	2.16×10^{-5}	2.44×10^{-3}	2.13×10^{-3}
$u_0\delta/\nu$		463	615	707

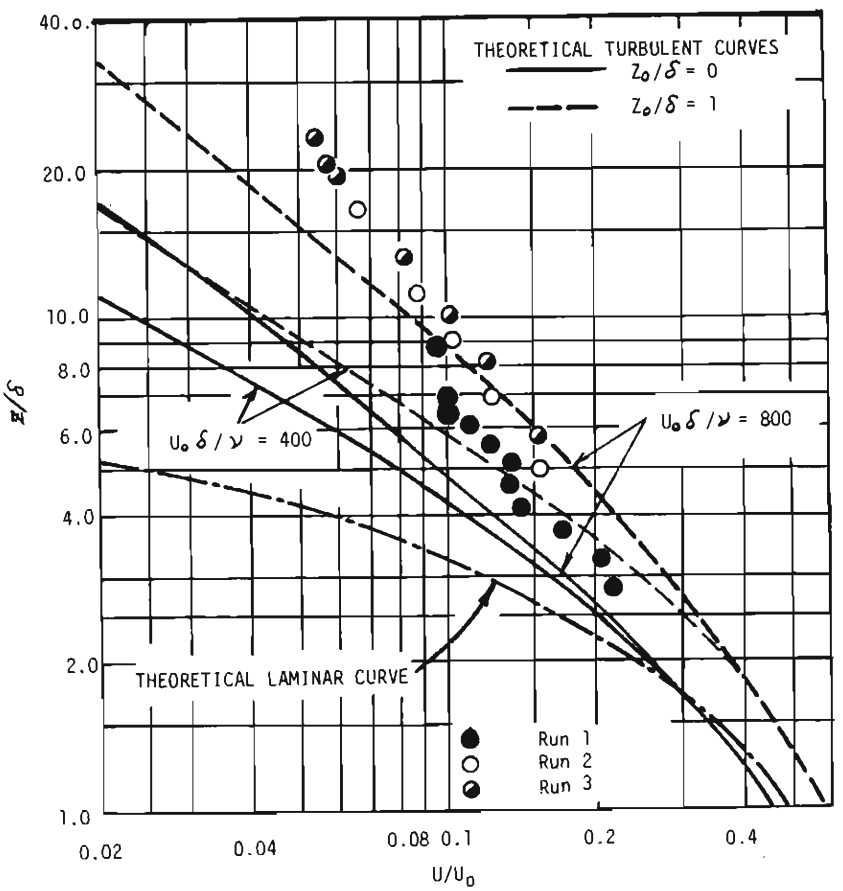

Fig. 5. Comparison of the observed velocity profiles with the theoretical one (after Kalkanis).

Kalkanis measured the velocity distribution in a turbulent oscillatory flow over smooth and rough platforms which oscillated with a simple harmonic motion. In all of his experiments, the amplitude A_B of the moving platform and its period $T=2\pi/\omega$ were chosen to insure conditions of turbulent flow, so the maximum velocity of the platform u_0 is equal to $A_B\omega$. The velocity was measured by a symmetric instrument similar to a Pitot tube combined with an electric indicater for measuring pressure differences. His experimental conditions for the smooth platform are presented in Table 2.

On the other hand, the theoretical velocity profile induced by the periodic oscillation of a platform at the bottom is given by Eq. (22):

$$u = u_0 F(\xi) e^{i\omega t} \tag{71}$$

where $\xi_0=1$ for the smooth bottom. Therefore, $F(\xi)$ for this case may be computed by using Eq. (29), (36) and (41) and putting $z_1/\delta=50$, $z_3/\delta=100$ and $\alpha=(u_0\delta/\nu)\times10^{-3}$. Figure 5 shows the comparison of the observed theoretical one indicated by the full and broken lines, respectively.

Although the scatter of points can be seen, this figure indicates that the experimental values shown by Kalkanis are generally more than those predicted by the theory. However, the trend of the experimental values in which u/u_0 increases with the increasing of the Reynolds number is in agreement with the theory. It seems that the deviation causes the structure of the turbulence over the oscillating plate to be different from that produced by the oscillatory body of water.

3. Mass Transport by Oscillatory Flow in the Turbulent Boundary Layers

(1) Formulation

Using the well-known values of Longuet-Higgins[10], the mass transport velocity within the bottom boundary layer is defined by the real part of

$$\overline{U} = \varepsilon^2\left\{\overline{u_2} + \overline{\int u_1 dt \cdot \frac{\partial u_1}{\partial x}} - \overline{\int\left(\int_{\xi_0}^{\xi}\frac{\partial u_1}{\partial x}\,d\xi\right)dt\,\frac{\partial u_1}{\partial \xi}}\right\} \tag{72}$$

where the overbar denotes the average over one wave period and u_1 is already solved in the preceding section. However, the second-order velocity u_2 is not well understood. From Eqs. (13) and (14), the differential equation of the second approximation for u is given by the expression:

$$\frac{\partial u_2}{\partial t} + u_1\frac{\partial u_1}{\partial x} - \frac{\partial u_1}{\partial \xi}\int_{\xi_0}^{\xi}\frac{\partial u_1}{\partial x}d\xi = \frac{\partial u_{\infty 2}}{\partial t} + u_{\infty 1}\frac{\partial u_{\infty 1}}{\partial x} + \alpha^2\omega\frac{\partial}{\partial \xi}\left(N\frac{\partial u_2}{\partial \xi}\right) \tag{73}$$

As shown by Schlichting[11], since the second-order velocity u_2 has an oscillatory component u_{2p} in addition to a time-independent component u_{2s}, then

$$\overline{u}_2 = u_{2s}.$$

The boundary conditions for Eq. (73) can be written as:

$$u_{2p} = u_{2s} = 0 \qquad \text{at} \quad \xi = \xi_0 \tag{74}$$

$$\left.\begin{aligned} &u_{2p} = u_{\infty 2} \\ &u_{2s}: \text{finite}, \quad \frac{\partial u_{2s}}{\partial \xi} = 0 \end{aligned}\right\} \quad \text{at} \quad \xi\to\infty \tag{75}$$

The purpose of this section is not solve the second-order velocity u_2, but is to compute the mass transport velocity. Thus, it is found from Eq. (73) that only a solution for $\overline{u}_2$ is required. The time average of Eq. (73) over one wave period is given by

$$\overline{u_1\frac{\partial u_1}{\partial x}}-\frac{\partial \bar{u}_1}{\partial \xi}\int_{\xi_0}^{\xi}\overline{\frac{\partial u_1}{\partial x}}\,d\xi=\overline{u_{\infty 1}\frac{\partial u_{\infty 1}}{\partial x}}+\alpha^2\omega\frac{\partial}{\partial \xi}\left(N\frac{\partial \bar{u}_2}{\partial \xi}\right) \tag{76}$$

Substituting Eq. (17) into Eq. (76) yields

$$2\alpha^2\omega\frac{\partial}{\partial \xi}\left(N\frac{\partial \bar{u}_2}{\partial \xi}\right)=u_{b1}^*\frac{du_{b1}}{dx}\left[FF^*-(F+F^*)+\frac{dF^*}{d\xi}(\xi-\xi_0-\int_{\xi_0}^{\xi}Fd\xi\right] \tag{77}$$

in which the asterisk denotes the complex conjugate and only the real part of $\bar{u}_2$ is to be retained, because only that of u_1 is significant. If the time average velocity u_2 is defined in the form :

$$\bar{u}_2=\frac{1}{2\alpha_2\omega}u_{b1}^*\frac{du_{b1}}{dx}G(\xi) \tag{78}$$

with boundary conditions

$$\begin{aligned} &G(\xi)=0 \qquad \text{at} \quad \xi=\xi_0\\ &G(\infty) : \text{finite}\\ &dG/d\xi=0 \qquad \text{as} \quad \xi\to\infty \end{aligned} \tag{79}$$

then

$$\frac{d}{d\xi}\left(N\frac{dG}{d\xi}\right)=FF^*-(F+F^*)+\frac{dF^*}{d\xi}\left(\xi-\xi_0-\int_{\xi_0}^{\xi}Fd\xi\right) \tag{80}$$

(2) Analytical solution

The integration of Eq. (18) with respect to ξ yields

$$\int_{\xi_0}^{\xi}Fd\xi=i\alpha^2\left\{\xi_0^2F'(\xi_0)-N\frac{dF}{d\xi}\right\} \tag{81}$$

Therefore, substituting Eq. (81) into Eq. (80) and taking $F(\xi_0)=1$ and $F(\infty)=0$ into account gives

$$\frac{d}{d\xi}\left(N\frac{dG}{d\xi}\right)=FF^*-(F+F^*)+(\xi-\xi_0)\frac{dF}{d\xi}+i\alpha^2\frac{dF^*}{d\xi}\times\left\{N\frac{dF}{d\xi}-\xi_0^2F'(\xi_0)\right\} \tag{82}$$

Integrating this equation from ξ_0 to ξ, and taking the boundary conditions into account :

$$\begin{aligned} N\frac{dG}{d\xi}=&\xi_0^2G'(\xi_0)+\int_{\xi_0}^{\xi}FF^*d\xi-2\alpha^2\mathrm{Im}\left[N\frac{dF}{d\xi}-\xi_0^2F'(\xi_0)\right]\\ &+\int_{\xi_0}^{\xi}\xi\frac{dF^*}{d\xi}d\xi-\xi_0(F^*-1)-i\alpha^2\xi_0^2F'(\xi_0)(F^*-1)\\ &+i\alpha^2\int_{\xi_0}^{\xi}N\frac{dF}{d\xi}\frac{dF^*}{d\xi}d\xi \end{aligned} \tag{83}$$

where the symbol Im denotes the imaginary part of the value in the brackets.

The last term of the right-hand side of Eq. (83) may be integrated by parts. This yields

$$\int_{\xi_0}^{\xi}N\frac{dF}{d\xi}\frac{dF^*}{d\xi}d\xi=NF^*\frac{dF}{d\xi}-\xi_0^2F'(\xi_0)-\frac{i}{\alpha^2}\int_{\xi_0}^{\xi}FF^*\,d\xi \tag{84}$$

Furthermore, from Eq. (84) it follows that

$$\int_{\xi_0}^{\xi}N\frac{dF}{d\xi}\frac{dF^*}{d\xi}d\xi=\mathrm{R}\left[NF^*\frac{dF}{d\xi}-\xi_0^2F'(\xi_0)\right] \tag{85}$$

and

$$\int_{\xi_0}^{\xi}FF^*d\xi=\left[\alpha^2\mathrm{Im}NF^*\frac{dF}{d\xi}-\xi_0^2F'(\xi_0)\right] \tag{86}$$

finally, substituting these expressions into Eq. (83) gives the equation for G :

$$N\frac{dG}{d\xi}=\xi_0^2G'(\xi_0)-2\alpha^2\mathrm{Im}\left[N\frac{dF}{d\xi}(1-F^*)\right]+(\xi-\xi_0)F^*$$
$$-i\alpha^2\left[N\frac{dF_*}{d\xi}-\xi_0^2\{F'(\xi_0)\}^*-N\frac{dF}{d\xi}F^*-\xi_0^2F^*F'(\xi_0)\right] \quad (87)$$

Since this equation must satisfy the boundary conditions, $dG/d\xi=0$ and $F=0$ as $\xi\to\infty$, the first term of the right-hand side of this equation must be written by :

$$\xi_0^2G'(\xi_0)=-i\alpha^2\{F'(\xi_0)\}^*$$

Therefore,

$$N\frac{dG}{d\xi}=2\alpha^2\mathrm{Im}\left[N\frac{dF}{d\xi}F^*-N\frac{dF}{d\xi}\right]+(\xi-\xi_0)F^*-i\alpha^2N\frac{dF^*}{d\xi}$$
$$+i\alpha^2\left\{NF^*\frac{dF}{d\xi}-\xi_0^2F^*F'(\xi_0)\right\} \quad (88)$$

Moreover, an integration of the above equation by taking $G(0)=0$ into account yields

$$G(\xi)=i\alpha^2\Big(FF^*+F-2F^*)-\int_{\xi_0}^{\xi}F^*\frac{dF}{d\xi}d\xi$$
$$-\int_{\xi_0}^{\xi}(F^*/N)\{\xi_0^2F'(\xi_0)+(i/\alpha^2)(\xi-\xi_0)\}d\xi \quad (89)$$

Using the mass transport velocity defined as follows :

$$\bar{U}=\frac{\varepsilon^2}{2\alpha^2\omega}u_{b1}^*\frac{du_{b1}}{dx}K(\xi), \quad (90)$$

and substituting Eqs. (88) and (89) into Eq. (72), the non-dimensional form of Eq. (72) can be expressed by :

$$K(\xi)=i\alpha^2\left[2FF^*-3F^*+1-(\xi-\xi_0)\frac{dF^*}{d\xi}-\int_{\xi_0}^{\xi}F^*\left\{\frac{dF}{d\xi}+\frac{\xi_0^2F'(\xi_0)}{N}\right\}d\xi\right]$$
$$+\alpha^4\frac{dF^*}{d\xi}\left\{N\frac{dF}{d\xi}-\xi_0^2F'(\xi_0)\right\}+\int_{\xi_0}^{\xi}\frac{(\xi-\xi_0)F^*}{N}d\xi \quad (91)$$

(3) Numerical values and comparison with experimental data

The vertical distribution of the mass transport velocity in the turbulent boundary layers induced by surface waves can be evaluated by obtaining a numerical solution of Eq. (91). In order to generalize the theoretical description of the mass transport within the bottom turbulent boundary layer under wave action, it is convenient to deal with partial reflected waves.

The surface elevation for the partial reflected waves is given by the form of the real part of

$$\eta=\frac{H_i}{2}i(e^{-ikx}+re^{ikx})e^{i\omega t}$$

where H_i is the incident wave height and r the reflection coefficient. The bottom velocity corresponding to this is

$$\varepsilon u_{\infty 1}=\varepsilon u_{b1}e^{i\omega t} \quad (92)$$

and

$$u_{b1}=(u_0/\varepsilon)\,i\,(e^{-ikx}-re^{ikx}) \quad (93)$$

where

$$u_0=\pi H_i/T\sinh kh$$

It is evident that only the real part of these expression has significance. Now, it is asumed that

$$K=\alpha^2(K_{st}+iK_{pt}) \quad (94)$$

in which K_{st} and K_{pt} are the real and imaginary part of K, respectively. From (93), the complex conjugate of u_{b1} and the derivative of u_{b1} with x are given by :

$$u_{b1}^{*} = -(u_0/\varepsilon)\, i\,(e^{ikx} - re^{-ikx}) \tag{95}$$

and

$$du_{b1}/dx = (u_0/\varepsilon)\, k\,(e^{-ikx} + re^{ikx}) \tag{96}$$

By substituting these expressions into Eq. (90), the mass transport velocity is given by :

$$\bar{U} = \frac{1}{2}\left(\frac{k}{\omega}\right)u_0^2\{-i(1-r^2)+2r\sin 2kx\}(K_{st}+iK_{pt})$$

and finally, retaining the real part of this equation yields

$$\bar{U} = \frac{1}{2}\left(\frac{k}{\omega}\right)u_0^2\{(1-r^2)K_{pt}+2rK_{st}\sin 2kx\} \tag{97}$$

According to Longuet-Higgins, the mass transport velocity obtained by laminar theory is expressed by

$$\bar{U}_L = \frac{1}{4}\left(\frac{k}{\omega}\right)u_0^2\{(1-r^2)K_{pt}+2rK_{st}\sin 2kx\} \tag{98}$$

The comparison of Eq. (97) with Eq. (98) indicates that the mass transport described by the turbulent theory is formally similar to that of the laminar one. As is evident from Eq. (97), since $r=0$ and $r=1$, it is found that K_{pt} and K_{st} describe the vertical distributions of the mass transport velocity within the turbulent boundary layer in the case of a progressive wave and of a standing wave, respectively.

In general, it is very complicated and slow to compute the values of K numerically, so it is necessary to simplify the computation of Eq. (91), For this, the nondimensional form of the mass transport velocity is approximated as follows :

$$K(\xi) \approx i\alpha^2\left[\, 2FF^{*}-3F^{*}+1-(\xi-\xi_0)\frac{dF^{*}}{d\xi}-\int_{\xi_0}^{\xi} F^{*}\frac{dF}{d\xi}\,d\xi\,\right] \tag{99}$$

Figure 6 (a) and (b) show the variations of K_{pt} and K_{st} with z/δ calculated for the case of $z_0/\delta = 0$ and the various values of $Re(=u_0\delta/\nu)$, respectively. In these figures, the dotted lines describe the velocity profiles of the mass transport according to the laminar theory. It is found that the velocity profiles for the turbulent boundary layer over smooth bottom vary slightly with the increasing

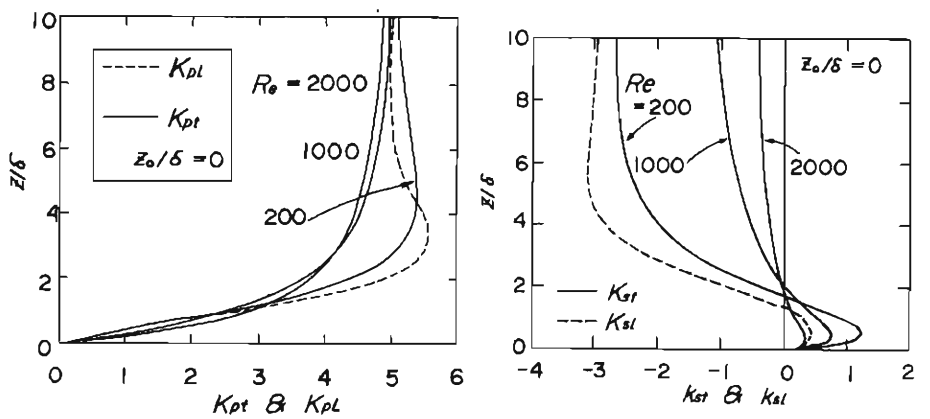

Fig. 6. Variations of K_{pt} and K_{st} with z/δ.

of the values of Re. However, the effect of the Reynolds number on the values of K_{pt} is not remarkable in the range of $Re \leq 2000$, and also the values of K_{pt} are little different from those predicted by the laminar theory.

On the other hand, it is found that the values of K_{st} decrease considerably

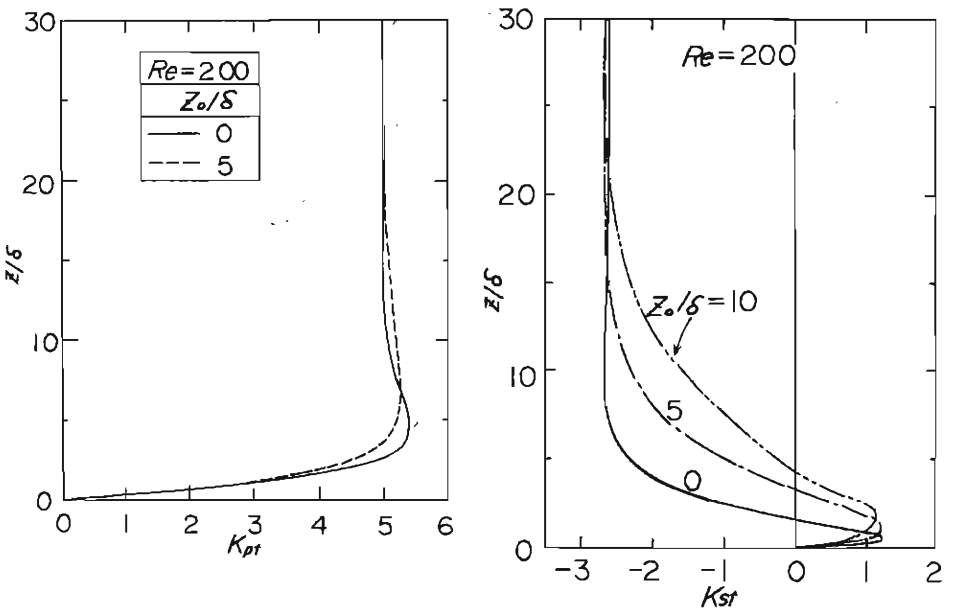

Fig. 7. The effect of roughness on the values of K_{pt} and K_{st}.

with the increasing of the Reynolds number. In addition, an outstanding feature which this figure shows is that the transport in the lower layer for the range of $z/\delta < 2.0$ is contrary to that in the upper one.

Figures 7 (a) and (b) show the variations of K_{pt} and k_{st} with z/δ computed for the case of $Re = 200$ and the various values of z_0/δ, respectively.

It is evident from these figures that the effect of roughness on standing waves is greater than its effect on progressive waves.

Figure 8 shows the variation of K_{st} with z/δ calculated for the various values of Re in the case of a rough bottom ($z_0/\delta=5$). A comparison between the cases of smooth and rough bottoms indicates that the thickness of the reverse transport layer increases

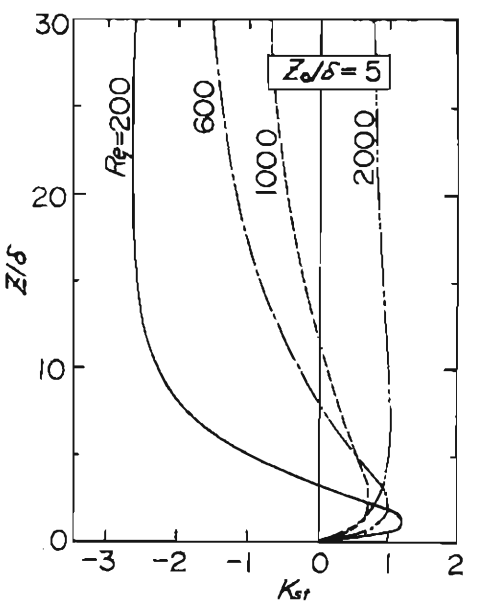

Fig. 8. Relationship between K_{st} and Re.

with the increasing of the Reynolds number. Furthermore, Figure 9 shows the relationship between the values of K_{st} and those of z_0/δ. It is also found that the thickness of the reverse transport layer increases with the increasing of the roughness length similar to that of the Reynolds number.

Figure 10 shows a comparison between experimental values and the theoretical curves for mass transport velocity change in x direction. In these figures, the full and dotted lines describe the theoretical curves computed by laminar and turbulent theories, respectively. Measurements of the mass transport velocity were made by using nylon particles with a diameter of 4.8 mm and a specific gravity of 1.10. Although agreement between the experimental values and the theoretical curves is very poor, the maximum values of the experimental results are roughly in agreement with the dotted curves obtained by turbulent theory.

This may be due to the velocity difference between the nylon and water particles. The application of the above data to the problem of sediment movement induced by wave motion is important, since the direction of sediment movement may be determined by the existence of the mass transport.

In general, the order of the mass transport velocity is higher than that of the oscillatory velocity of water particles and its magnitude is generally small, but it is possible that bottom materials are transported by the composite flows. Therefore, it seems that the direction of the drifting sand is determined by that of the mass transport in the boundary layer. From this prediction, it seems that beach processes in prototype and model are influenced by the mass transport within the boundary layer. Therefore, a point to which special attention should be paid is that the values of Re and z_0/δ play an important role with respect to the scale effect of beach processes.

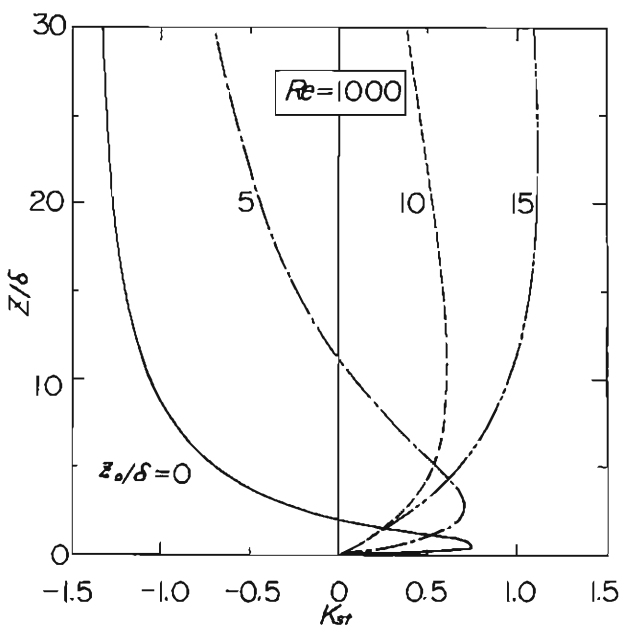

Fig. 9. Relationship between K_{st} and z_0/δ.

4. Conclusion

I have studies fluid motion in the turbulent boundary layers developed on smooth and rough bottoms under wave motion, especially the velocity profile and the mass transport velocity in the boundary layers.

The followng conclusions may be derived from the results of this study :

1) The velocity profile of an oscillatory flow in a turbulent boundary layer observed by Jonsson agrees with the theoretical value except for the large value of z/δ. However, the experimental values obtained by Kalkanis are not in agreement with the theoretical curves.

2) The computation of the mass transport velocity presented here is an application of the turbulent boundary layer theory. The outstanding feature of the numerical results for the mass transport velocity is that its velocity profile for standing waves is greater in the laminar case than in the turbulent case.

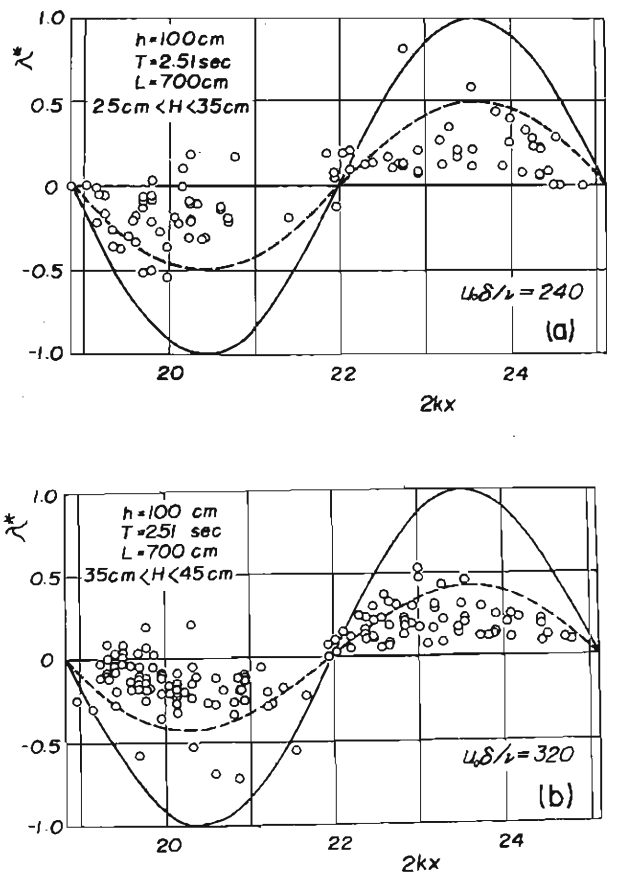

Fig. 10. Comparisons between experimental results and theoretical curves.

3) The direction of the mass transport velocity for standing waves is influenced by the bottom roughness. Therefore, it is possible that the direction of the net sediment movement is different according to the scale of characteristics of wave and sediment.

Acknowledgments

The author wishes to express his great appreciation to prof. Y. Iwagaki for his valuable suggestions in carrying out this study and to prof. Y. Tsuchiya for his encouragement in the preparation of this paper.

References

1) Longuet-Higgins, M. S. : The mechanics of the boundary layer near the bottom in a progressive wave, proc. of 6th Conf. on Coastal Engg., 1958, pp. 184-194.
2) Iwagaki, Y. and Y. Tsuchiya : Laminer damping of oscillatory wave due to bottom friction, proc. of 10th Conf. on Coastal Engg., 1966, pp. 149-174.
3) Kalkanis, G. : Turbulent flow near an oscillating wall, B. E. B. Tech. Memo. No. 97, 1957, 36p.
4) Jonsson, I. G. : measurements in the turbulent wave boundary layer, 10th Congress of IAHR, 1963, pp. 85-92.
5) Horikawa, K. and A. Watanabe : Experimental studies on oscillatory boundary layers due to surface waves, Proc. of 15th Conf. of Coastal Engg. in Japan, 1965, pp. 16-23.
6) Kajiura, K. : A model of the bottom boundary layer in water waves, Bull. Earthq. Res. Inst., Vol. 46, 1968, pp. 75-123.
7) Johns, B. : The damping of gravity waves in shallow water by energy dissipation in a turbulent boundary layer, Tellus xx, No. 2, 1968, pp. 320-337.
8) Carlsen, N. A. : Measurements in the turbulent wave boundary layer, Basic Res. Progress Report 14, Coastal Engg. Lab., Tech. Univ. of Denmark, 1967, pp. 2-3.
9) Iwagaki, Y. and I. Chen : Experimental studies on bottom friction due to waves in the range of transition, D. P. R. I. Annuals, No. 11 B, 1968, pp. 355-374.
10) Longuet-Higgins, M. S. : Mass transport in waves, Phil. Tran. Royal Soc., London, Series A. No. 903, 1953, pp. 535-581.
11) Schlichting, H. : Boundary layer theory, translated by Kestin, J., McGraw-Hill, Series in Mechanical Engg., 1960, pp. 207-229.